Evaluation of identification method of the fluid/structure interaction forces in turbo machine levitated by active magnetic bearings

Tea-Jin PARK, Yoichi KANEMITSU and Shinya KIJIMOTO

Dept.of Intelligent Machinery and Systems, Graduate school, Kyushu University,

6-10-1,Hakozaki, Higashi-ku, Fukuoka, Japan 812-8581

tjpark@sky.mech.kyushu-u.ac.jp

Abstract

In this research, in addition to the mass unbalance and high order sensor runout, the fluid/structure interaction forces are identified with the recursive least square method. We identify the fluid force generated in the turbo machine and apply to the control of the rotor vibration using the identified result. A series of simulations and experiments are carried out. Then, the proposed identification method in this research is proved to utilize to the estimation of the fluid force effectively. An overhung rotor of a turbo molecular vacuum pump was used as the experimental apparatus.

Introduction

The active magnetic bearing controls the electromagnetic field, which levitates and supports the rotor without physical contact. The mass unbalance of the rotor is caused by machining accuracy and assembling tolerance. And it is a dominant source of synchronous whirling of the rotor. Therefore, if the unbalance force that acts on the rotor is compensated using the electromagnetic force from the rotor levitated by active magnetic bearings (AMBs), a whirl motion of the rotor becomes smaller or disappears.

A turbo machine is related in various shapes to the fluid. For instance, a journal bearing supports a rotor using the pressure of oil and the gas. A turbine rotates its rotor by the force of the gas, steam or water. Moreover, a pump throws water by rotating the impeller.

In general, the fluid causes the damping action to the rotor. Because of the generating the self-excited vibration in the rotor by various mechanisms, the fluid in the rotation field occasionally causes accidents, which are not forecasted. Moreover, the fluid that entered in the hollow shaft becomes an unbalance and causes the forced vibration. These fluid/structure interaction forces are generated at the annular clearances, the mechanical seals, the inside of impellers and the impeller tip and shroud, which heavily affect the rotor dynamic behaviors. The generation mechanism should be understood enough to prevent such a vibration, and appropriate countermeasures should be considered. The fluid forces by the interaction between the fluid and the structure can be classified into pure excitation forces and motion dependent forces.

In the experiments, the fluid/structure interaction forces, which correspond to the fluid force generated in the turbo machine, are calculated in proportion to measured displacement in consideration of both the spring coefficient and the damping coefficient. The calculated values are fed back to the non-contact magnetic excitation apparatus. The magnetic pull forces, which are proportional to the fluid/structure interaction forces, act on the apparatus rotor. The motion dependent forces are identified by the proposed experimental method as above mentioned. And we conduct identification experiments on the mass unbalance and the fluid/structure interaction forces, using the measured data of shaft vibration data caused by excitation force and unbalance.

Magnetic exciter

The fluid force, which has generated in the turbo machine, is simulated with the magnetic excitation apparatus. A magnetic bearing supports the rotor by non-contact using the magnetic attractive force generated by the electromagnet. In this research, we propose the magnetic circuit model of the idealized eight-pole type radial magnetic bearing. And the magnetic attractive force is derived based on the model.

The magnetic excitation machine is composed only of the electromagnet. The layered product of the silicon steel sheet, which is ferromagnetic, is used

for the magnetic pole part of the electromagnet. Figure 1 is a cross section when the coil is installed in the magnetic pole of eight-pole type radial magnetic bearing.

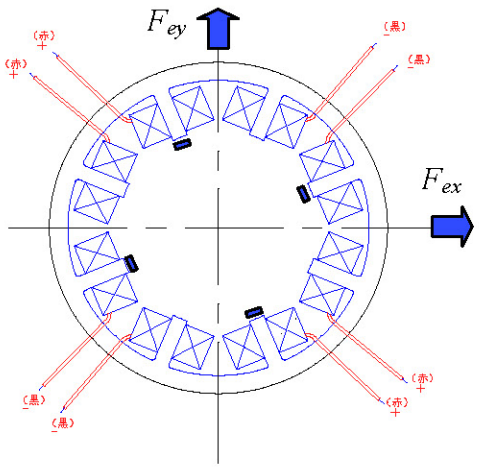

Fig.1 8 poles magnetic bearing

In idealized condition and magnetic circuit model, when the relational expression of the flux is led by using the Kirchhoff's laws, it is expressed as follows.

$$NI = \phi R \tag{1}$$

Where N, I, ϕ, R are number of turns, a bias current in each coil, a magnetic flux, a magnetic reluctance in the state of equilibrium respectively. This reluctance is shown as follows by vacuum magnetic permeability μ_0, radius clearance C_r between the magnetic pole and rotor in the equilibrium position, and magnetic pole sectional area S:

$$R = \frac{C_r}{\mu_0 S} \tag{2}$$

The magnetic flux can be shown from equation (1) and equation (2) as follows:

$$\phi = \frac{\mu_0 SNI}{C_r} \tag{3}$$

In the equilibrium state, magnetic attractive forces F_{ex}, F_{ey} generated in the direction of x and y is expressed using the magnetic flux density B as follows:.

$$F_{ex} = 2 \times \frac{\phi^2}{2S\mu_0} \cos 22.5 = 2 \times \frac{B^2 S}{2\mu_0} \cos 22.5 \tag{4a}$$

$$F_{ey} = 2 \times \frac{\phi^2}{2S\mu_0} \cos 22.5 = 2 \times \frac{B^2 S}{2\mu_0} \cos 22.5 \tag{4b}$$

The magnetic attractive force of a magnetic exciter depends on the magnetic flux density of the gap on the rotor and the magnetic pole. As for the limitation of the exciter force, when the magnetic flux density is adjusted to 1T, the stress from the force magnetic pole 0.4-0.5[MPa] is appropriate to the per projection area of the magnetic pole in a magnetic bearing.

In this research, the magnetic exciter, which generates the magnetic attractive force of 50[N] in the x direction, is designed and made under the design condition described in Table 1.

Table 1 Design parameters

Parameter	Value
Rotor Diameter	D_{rot} = 63.44 [mm]
Inner Diameter of Radial AMB	D_{in} = 65.0[mm]
Width of Radial AMB	L_{AMB} = 64.4 [mm]
Radial Clearance	C_r = 0.78 [mm]
Diameter of Magnet Wire	d_w = 0.6 [mm]
Maximum Current	I_{max} = 4 [A]
Maximum Flux Density	B = 1.2 [T]

When the excitation force is set to 50[N] from equation (4), the area of the magnetic pole is calculated as follows:

$$S = \frac{50 \times \mu}{B^2 \times \cos 22.5} = 47 \times 10^{-6} \text{ [m}^2\text{]} \tag{5}$$

In this research, the magnetic exciter is 5mm in width of the magnetic pole, 10mm in length, 4[A] in the current of the bias, and the radius clearance is designed to be 0.78mm. As a result, the number of coil turns becomes 186 from equation (5), (6). Then the magnetizing force is given as follows:

$$NI = \phi R = \frac{BC_r}{\mu} = \frac{1.2 \times 0.78 \times 10^{-3}}{4\pi \times 10^{-7}} = 744.8 \tag{6}$$

To insert this coil between magnetic poles, the sectional space area A for coil is calculated by space factor (fw=0.545) of the coil and above-mentioned condition.

$$A = \frac{\pi d^2 N}{4 \cdot f_w} = \frac{\pi \times 0.8^2 \times 155}{4 \times 0.545} = 142.9 \text{ [mm}^2\text{]} \tag{7}$$

And the magnetic attractive force is calculated as follows by the use of the sectional area S of poles as follows:

$$\begin{aligned} F_{ey} &= 2 \times \frac{\phi^2}{2S\mu} \cos 22.5 = 2 \times \frac{B^2 S}{2\mu} \cos 22.5 \\ &= \frac{1.2^2 \times 50 \times 10^{-6}}{4\pi \times 10^{-7}} \cos 22.5 = 57.3 \text{[N]} \end{aligned} \tag{8}$$

The magnetic exciter has been made with the shape shown in Table 2 by the above-mentioned design.

Table 2 Result of design parameters

Parameter	Value
Magnetic pole area	S=50[mm^2]
Magnetic pole width	w=5[mm]
Magnetic pole height	h=10[mm]
Turn no. of coil	N=186[-]

Modeling

The fluid force F_{fx} and F_{fy} are expressed like equation (9) as used by the model of a journal bearing and an annular seal.

$$-\begin{Bmatrix} F_{fx} \\ F_{fy} \end{Bmatrix} = \begin{bmatrix} c_{xx} & c_{xy} \\ c_{yx} & c_{yy} \end{bmatrix} \begin{bmatrix} \dot{x}_e \\ \dot{y}_e \end{bmatrix} + \begin{bmatrix} k_{xx} & k_{xy} \\ k_{yx} & k_{yy} \end{bmatrix} \begin{bmatrix} x_e \\ y_e \end{bmatrix} \quad (9)$$

where x_e, y_e are displacements of the rotor at the exciter position. Equation of motion of the rigid rotor shown in figure 2 and levitated by 2 AMBs is given as following equation.

$$M\ddot{x} + \omega M_1 \dot{x} = U - Fi + Gx_s + C\dot{x} + Kx \quad (10)$$

where M, M_1, U, F, G, C, K are the mass matrix, the gyro-moment matrix, the rotor unbalance matrix, the control stiffness matrix, the negative position stiffness matrix, the damping coefficient matrix and the spring coefficient matrix.

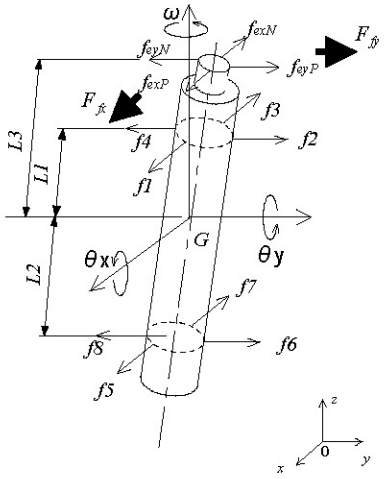

Fig. 2 model of rotor

The recursive least square method is applied to equation (10). [2,3]

Table 3 Initial parameter of simulation

Static unbalance: ε	30.0[μm],
Static unbalance phase: α	1.0[rad]
Dynamic unbalance: τ	200[μrad]
Dynamic unbalance phase: β	-0.5[rad]
Damping coefficient: c, c_c	0.05, 0.05[Ns/m]
Spring coefficient: k, k_c	787, -2.7[N/m]

Test rig

Figure 3 shows the experimental apparatus for evaluating the proposed identification method of the fluid/structure interaction forces. The exciter rotor was assembled on the top of rotor in a turbo molecular vacuum pump (TMP). The apparatus uses vertical overhung rotor of the TMP. The rotor is supported by two AMB, namely the upper AMB and lower AMB. The AMB's have two proximity sensors in orthogonal directions x-y to measure and regulate the relative displacements between the rotor and the stator. The AMB analog controllers consist of sensor boards, PID controllers and PWM power amplifiers. The outputs from the sensor boards, which are proportional to the relative displacements, are connected to the A/D converters. The real time operating system RT-Linux is running the host computer.

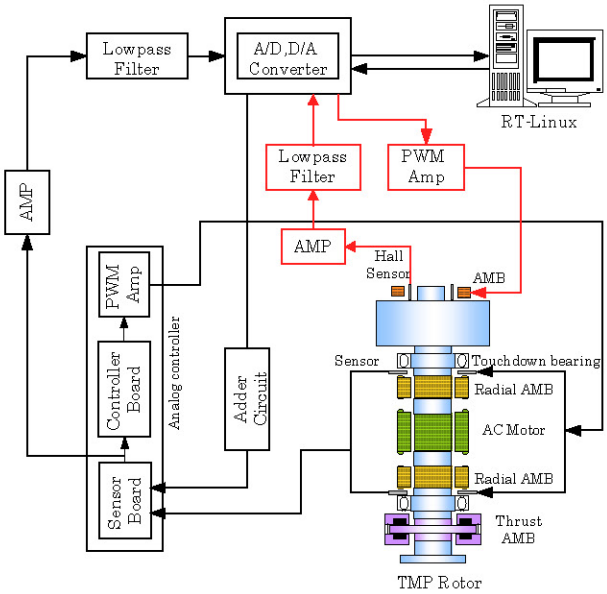

Fig. 3 Apparatus of TMP

The rotor is 204.3mm in length, 2.596kg in total mass, 0.114kg· m^2 in radial moment of inertia, and 0.002 kg· m^2 in polar moment of inertia and has a dummy disk on the top to add a known unbalance to evaluate the accuracy of the identification method. The rotating speed is calculated from a pulse signal output once every rotation. The analog vibration data is converted to digital signals at the constant sampling frequency (200Hz). The data is transferred to the host computer.

Simulation

The spring coefficients and the damping coefficients of the fluid force are set as shown in Table 3. The rotating speeds were set at 500 rpm and 1500 rpm. The shaft vibration data by simulation are shown in figure 4 and figure 5. The sampling time is 500μs.

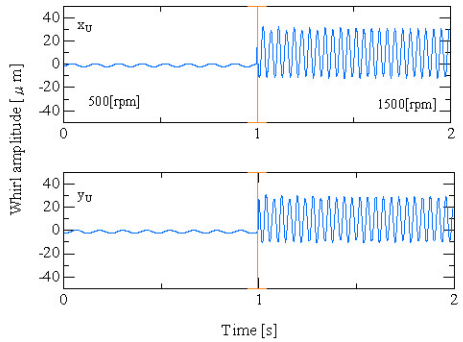

Fig.4 Whirling data from simulation at AMB U

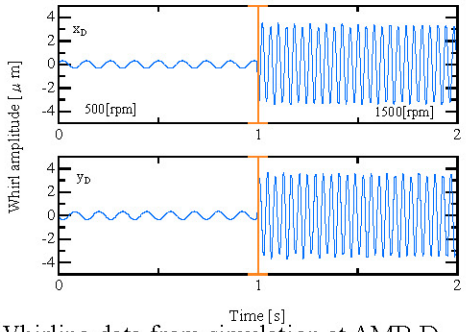

Fig.5 Whirling data from simulation at AMB D

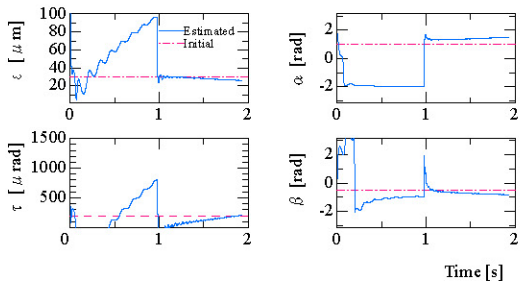

Fig.6 Estimated unbalance using the simulation whirl data

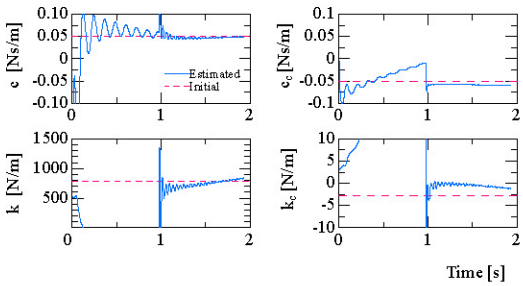

Fig. 7 Estimated spring coefficient and damping coefficient using the simulation whirl data

Figures 6, 7 show the identification process of mass unbalances, damping coefficients and spring coefficients. The identified static unbalance (ε) and dynamic unbalance (τ)are shown in figure 6. The left side figures and the right side figures show the amplitude and the phase angles of the unbalance. And the identified spring coefficients and damping coefficients of the fluid force are shown in figure 7. Thick solid lines indicate the result of the weighted least-square method, dot-dash lines are indicate the initial value. The static unbalance (ε) and phase angles of the identified parameters converge to the assumed values rapidly. But for the dynamic unbalance (τ), it takes more than 2 seconds to converge. The damping coefficient is converged to an initial value. However, The spring coefficient has taken 0.5 seconds or more for convergence.

Experiment

(1) Addition input signal

We conduct identification experiments on the mass unbalance and the fluid/structure interaction forces using the measured shaft vibration data added by excitation force and unbalance. The excitation forces, which are proportional to the fluid/ structure interaction forces, measured and calculated using the damping coefficient and spring coefficient. The calculated value generates the force which is proportional to fluid force by non-contacting magnetic exciter. The experiment was conducted at 1800rpm and 2500rpm. The damping coefficient and the spring coefficient, which are used for an addition signal, were assumed referring to the experiment of an annular gas labyrinth seal [4].

Damping coefficient c and spring coefficient k are given as an initial value and the addition signal is decided from the relation between equation (9) in case of $k_{xx} = k_{yy} = k$, $k_c = k_{xy} = 0$, $c_{xx} = c_{yy} = c$, $c_{xy} = c_{yx} = 0$.

Displacements x and y at the magnetic exciter position are calculated from the displacement measured with the displacement sensor of the magnetic bearings. And current i corresponding to the fluid force proportional to displacement is calculated from the displacement and the required fluid force. The excitation voltage is output from the D/A board to a magnetic exciter in consideration of the characteristic of the PWM amplifier.

The bias current N pole and P pole in the direction of y of the magnetic exciter is assumed to be I_N and I_P at the balance position. The change parts from the balance position value are assumed to be y_e and i_{ext}, and then electromagnetic power, which acts on the rotor, is as follows.

$$f_{fb} = -\frac{\mu_0 S N^2}{4}\left\{\frac{I_N}{C_r^{\,2}} + \frac{I_P}{C_r^{\,2}}\right\}\cdot i_{ext} + \frac{\mu_0 S N^2}{4}\left\{\frac{I_N^{\,2}}{C_r^{\,3}} + \frac{I_P^{\,2}}{C_r^{\,3}}\right\}\cdot y_e$$

$$= -F_{ext} i_{ext} + G_{ext} y_e \qquad (11)$$

where

$$F_{ext} = \frac{\mu_0 S N^2}{4}\left\{\frac{I_N}{C_r^{\,2}} + \frac{I_P}{C_r^{\,2}}\right\}$$

$$G_{ext} = \frac{\mu_0 SN^2}{4}\left\{\frac{I_N^{\ 2}}{C_r^{\ 3}} + \frac{I_P^{\ 2}}{C_r^{\ 3}}\right\}$$

C_r is a radius clearance at the balance position of the magnetic exciter. f_{ext} is electromagnetic force of the magnetic exciter. F_{ext}, G_{ext} are called magnetic exciter control stiffness and negative position stiffness respectively.

The current change part i_{ext} corresponding to the fluid force which is proportional to displacement from equation (12) is calculated as follows.

$$i_{ext} = \frac{G_{ext} \cdot y_e - F_{fy}}{F_{ext}} \qquad (12)$$

The additional current obtained from equation (12) is added to the bias currents in real time in N pole and P pole of the magnetic exciter. The variation of displacement at the exciter position of the rotor was shown in figure 8 and figure 12 by thick solid line. The voltage, which had been added at the 1800 rpm and 2500 rpm, was shown in figure 10, 11 and figure 14,15 respectively. Figure 9 and figure 13 show the excitation force calculated by displacement and the addition current. And displacement y_U and y_D in the direction of y at upper AMB and lower AMB were shown with the solid line and dotted line. When displacement, excitation force, and addition voltage are compared in these figures, it turns out that the voltage and excitation force are proportional to the displacement of rotor.

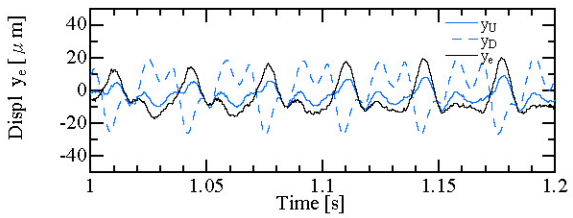

Fig.8 Displacement of y_e at 1800rpm

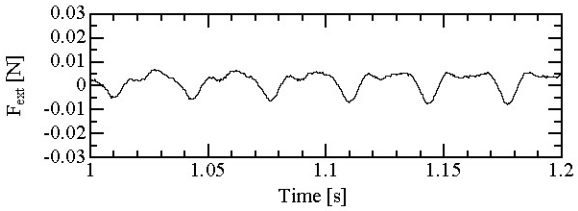

Fig.9 Excited force at 1800rpm

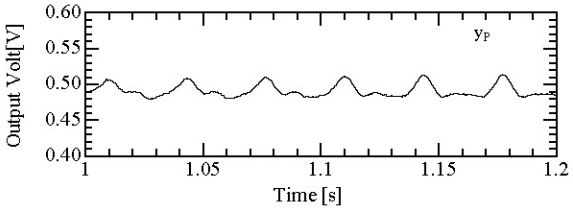

Fig.10 Output volt of the y_P pole at 1800rpm

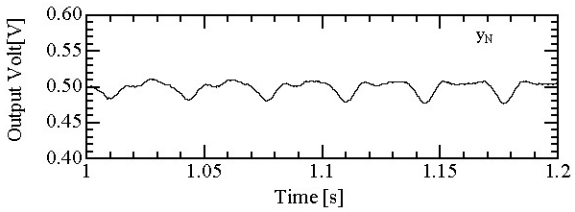

Fig.11 Output volt of the y_N pole at 1800rpm

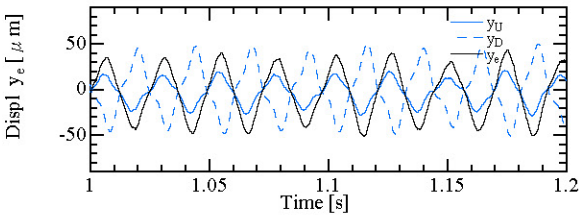

Fig.12 Displacement of y_e at 2500rpm

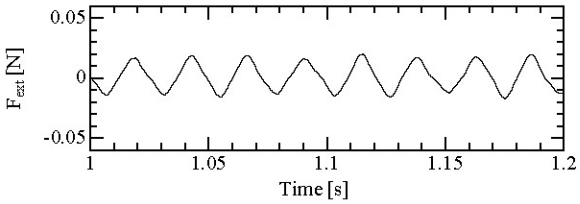

Fig.13 Excited force at 2500rpm

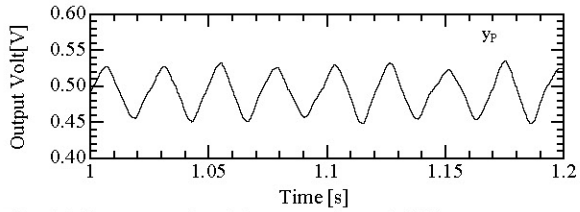

Fig.14 Output volt of the y_P pole at 2500rpm

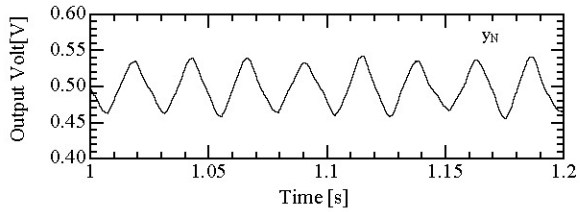

Fig.15 Output volt of the y_N pole at 2500rpm

(2) Rotor vibration data by addition input signal

Figure 16 shows the measured shaft vibration data at the 1800rpm and 2500rpm after assembling the rotor of exciter onto the apparatus rotor. The shaft vibration data is shown in figure 17 with y_U and y_D respectively when the excitation signal is added in the y direction of magnetic exciter. Moreover, the shaft vibration data y_U without the excitation signal in figure 16 was compared with the shaft vibration data y_U with excitation signal in figure 17, then we can see that the shaft vibration data with excitation signal are reduced by 10μm and 26μm in the p-p value, respectively. The amplitude has become smaller because of the spring coefficient.

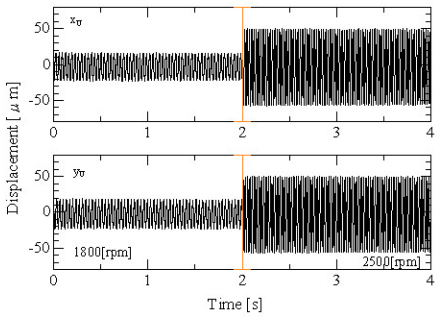

Fig. 16 Shaft vibration at AMB U without excitation force

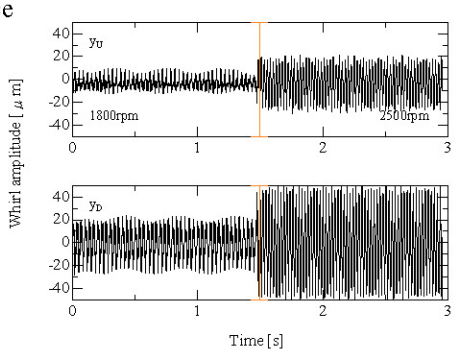

Fig. 17 Shaft vibration with added excitation force at AMB U ($c = 0.025\mathrm{N}\cdot\mathrm{s/m}, k = 393\mathrm{N/m}$)

(3) Experimental identification

Figure 18 and figure 19 show the identification result of the unbalance and fluid forces. The rotating speeds were set at 1800rpm and 2500rpm. Dot-dash lines in figure 18 indicate the damping coefficient and spring coefficient of the initial value, and the solid lines indicate the result of the identification. The damping coefficient c and the spring coefficient k converge to the initial values. The identification result of unbalance from measured shaft vibration signals are shown in figure 19. Dot-dash lines indicate the result of identified value after assembling the rotor of exciter onto the apparatus rotor, and the solid lines indicate the result of identified value using the measured shaft vibration data by added excitation signal. The identified result of unbalance from measured shaft vibration signals converges to the identification value of the residual unbalance, which identified after assembling. But amplitude of the static unbalance and the phase have some errors. The errors were caused by the undulation phenomenon in the shaft vibration data of figure 17.

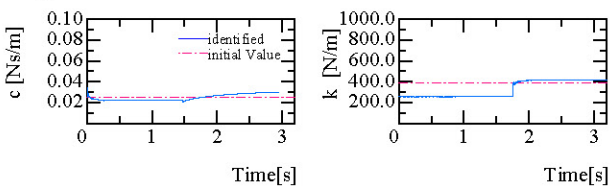

Fig.18 Estimated spring coefficient and damping coefficient using measured data

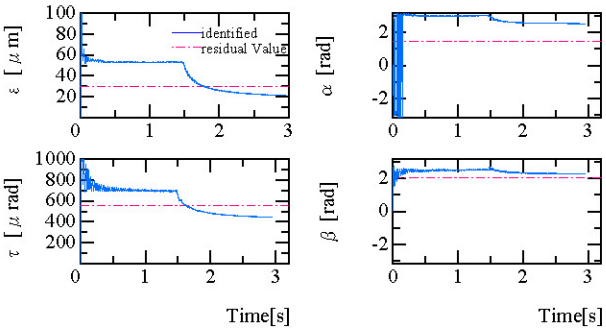

Fig.19 Estimated unbalance using measured data

Conclusions

1. In order to simulate the fluid force generated in the turbo machine, a magnetic exciter was designed and produced using electromagnets.
2. The unbalance and the motion dependent fluid force were identified by the numeric simulation and the experiment using the on-line recursive least square method.
3. The damping coefficient c and the spring coefficient k converge to the initial values.

References

[1] E. Knopf, R. Nordmann, Active Magnetic Bearings for the Identification of Dynamic Characteristics of Fluid Bearings-Calibration Result, Proc. of the 6th International Symposium on Magnetic Bearings, pp.52-61, 1998.

[2] Park, T.-J., Kanemitsu, Y., Kijimoto, S., and Matsuda, K., Identification of Unbalance and Sensor Runout on Rigid Rotor Supported by Magnetic Bearings(1st Report Identification by the incremental least square method), JSME, C, 66-652, pp113-119, 2000.

[3] Park, T.-J., Kanemitsu, Y., Kijimoto, S., and Matsuda, K., Identification of Unbalance and High Order Sensor Runout on Rigid Rotor Supported by Magnetic Bearings, Proc.of the 8th ISMB,pp355-360,2002.

[4] Dara Child, Turbomachinery Rotordynamics, Wiley Inter. Science, pp306-331

[5] Park, T.-J., Kanemitsu, Y., Kijimoto, S., and Matsuda, K., Evaluation of Identification Method of Sensor Runout by Using the Weighted Recursive Least Square Method, Proc. of the 7th International Symposium on Magnetic Suspension technology, pp. 191-196, 2003.